

# Reconstructing a light pseudoscalar in the Type-X Two Higgs Doublet Model

Eung Jin Chun,<sup>a</sup> Siddharth Dwivedi,<sup>b</sup> Tanmoy Mondal,<sup>b</sup> Biswarup Mukhopadhyaya<sup>b</sup>

<sup>a</sup>*Korea Institute for Advanced Study, Seoul 02455, Korea*

<sup>b</sup>*Regional Centre for Accelerator-based Particle Physics, Harish-Chandra Research Institute, HBNI, Chhatnag Road, Jhansi, Allahabad - 211 019, India*

*E-mail:* [ejchun@kias.re.kr](mailto:ejchun@kias.re.kr), [siddharthdwivedi@hri.res.in](mailto:siddharthdwivedi@hri.res.in),  
[tanmoymondal@hri.res.in](mailto:tanmoymondal@hri.res.in), [biswarup@hri.res.in](mailto:biswarup@hri.res.in)

**ABSTRACT:** We investigate the detectability as well as reconstructibility of a light pseudoscalar particle  $A$ , of mass in the 50 – 60 GeV range, which is still allowed in a Type-X (lepton-specific) two-Higgs doublet scenario. Such a pseudoscalar can be pair-produced in the decay  $h \rightarrow AA$  of the 125 GeV scalar  $h$ . The light pseudoscalar in the aforementioned range, helpful in explaining the muon anomalous magnetic moment, has not only substantial branching ratio in the  $\tau^+\tau^-$  channel but also one of about 0.35% in the  $\mu^+\mu^-$  final state. We show how to faithfully reconstruct the  $A$  mass using the  $\mu^+\mu^-$  mode, and establish the existence of a pseudoscalar around 50 – 60 GeV, using the process  $pp \rightarrow h \rightarrow AA \rightarrow \mu^+\mu^- \tau^+\tau^-$ . This is the most reliable way of reconstructing the light  $A$  mass, with a statistical significance that amounts to discovery, with a few hundred (or less)  $\text{fb}^{-1}$  of integrated luminosity.

**KEYWORDS:** Two Higgs Doublet Models, Higgs Physics, Extensions of Higgs sector, Beyond the Standard Model, LHC

---

## Contents

<b>1</b>	<b>Introduction</b>	<b>2</b>
<b>2</b>	<b>The Type-X 2HDM Model and Constraints</b>	<b>3</b>
<b>3</b>	<b>Signal of a light <math>A</math> : An analysis for the LHC</b>	<b>4</b>
3.1	Backgrounds	5
3.2	Simulation and event selection	6
<b>4</b>	<b>Results and Discussion</b>	<b>8</b>
<b>5</b>	<b>Summary and Conclusion</b>	<b>10</b>
<b>6</b>	<b>Acknowledgements</b>	<b>10</b>

---

# 1 Introduction

Extension of the electroweak symmetric sector of the standard model (SM) to two or more Higgs doublets is a widespread curiosity, of which two Higgs doublet models (2HDM) occupy the centre stage. Such models in general suffer from the flavour changing neutral current (FCNC) problem. A popular way of avoiding FCNC is to use some discrete symmetry (or something that effectively leads to it), which restricts the Yukawa interactions of the two doublets. Based on the nature of such symmetry, four types of 2HDM are popular, namely, Type-I, Type-II, Type-X (or lepton specific) and Type-Y (or flipped) [1–3]. This paper contains some observations related to Type-X 2HDM.

In this scenario, one scalar doublet in the flavour basis has Yukawa couplings with quarks only, while the other one couples to leptons alone (Yukawa coupling with neutrinos are neglected without affecting other aspects of phenomenology). The physical states other than the SM-like 125-GeV scalar, obtained on diagonalizing the mass matrices, have very small coupling with quarks compared to those with leptons, once all constraints including those from the Large Hadron Collider (LHC) are taken into account. This considerably relaxes the lower bounds on some of the physical masses. In particular, it has been found [4–6] that the neutral pseudoscalar  $A$  in Type-X 2HDM can be as light at 40–60 GeV or even lighter in certain regions in the parameter space, thanks to its generally low direct production rate at the LHC and other colliders that have run so far.<sup>1</sup> And it is in part of these regions where the one-loop contribution induced by a light  $A$  helps a good fit of the muon anomalous magnetic moment, especially for high ( $\geq 40$ ) values of  $\tan\beta$ , the ratio of the vacuum expectation values of the two doublets [10–14]. It is therefore important not only to look for LHC signals of this scenario [5], but also to *actually reconstruct the mass of the light  $A$* . We suggest a method of doing precisely that.

The light pseudoscalar, for large  $\tan\beta$ , has a  $\tau^+\tau^-$  branching ratio close to unity, and a  $\mu^+\mu^-$  branching ratio on the order of 0.35%. Signals have been suggested in the multi-tau channels like  $pp \rightarrow HA \rightarrow \tau^+\tau^- \tau^+\tau^-$  [5, 15–17]. However, the taus cannot be reconstructed in the collinear approximation [18] since there are four neutrinos in the final state. Besides, even if only one  $A$  decays into a  $\tau$ -pair, the visible  $\tau$ -decay product (like a  $\tau$ -induced jet) cannot be treated in the collinear approximation at such low energies as that possessed by the  $\tau$  produced from an  $A$  as light as 50 – 60 GeV. Therefore, we cannot reliably obtain  $m_A$  using the  $\tau$ -pair(s). We find that the  $\mu^+\mu^-$  pair can come to one’s rescue here. With  $pp \rightarrow hX \rightarrow AA \rightarrow \tau^+\tau^- \mu^+\mu^-$ , one may reconstruct  $m_A$  from the muon pair, in association with a pair of tau-jets. We show after a detailed simulation that such a strategy, combined with that for suppressing SM backgrounds, isolates the signal events carrying clear information on the pseudoscalar mass. It is thus possible to achieve discovery-level statistical significance with an integrated luminosity of about 100 fb<sup>-1</sup> or less at 14 TeV.

In Section 2 we discuss the generic features of the Type-X 2HDM with respect to the structure of the Yukawa and gauge couplings of the physical scalars and point out how the parameter space of the model gets constrained by the muon  $g-2$  and precision observables.

---

<sup>1</sup>Such light pseudoscalars may also occur in further extensions of the SM [7–9].

Section 3 is devoted to the the LHC analysis of our signal that identifies the pseudoscalar resonance, detailing the event selection criteria that helps in suppressing the backgrounds. Section 4 includes a discussion of the results in the context of the efficacy of the analysis scheme used for our signal. We summarize and conclude in Section 5.

## 2 The Type-X 2HDM Model and Constraints

The Type-X 2HDM with  $\Phi_{1,2}$  as the two doublets is characterised by the following Yukawa structure:

$$\mathcal{L}_Y = -Y^u \bar{Q}_L \tilde{\Phi}_2 u_R + Y^d \bar{Q}_L \Phi_2 d_R + Y^e \bar{L}_L \Phi_1 e_R + h.c., \quad (2.1)$$

where family indices are suppressed and  $\tilde{\Phi}_2 = i\sigma_2 \Phi_2^*$ . This Yukawa Lagrangian is the result of a  $\mathbb{Z}_2$  symmetry [19] which prevents tree level flavor changing neutral current. Under  $\mathbb{Z}_2$ , the fields transform as  $\Phi_2 \rightarrow \Phi_2$  and  $\Phi_1 \rightarrow -\Phi_1$  combined with  $e_R \rightarrow -e_R$  while the other fermions are even under it. Thus  $\Phi_2$  couples only to the quarks whereas  $\Phi_1$  couples exclusively to the leptons. The most general form of the scalar potential is

$$\begin{aligned} V_{2\text{HDM}} = & m_{11}^2 \Phi_1^\dagger \Phi_1 + m_{22}^2 \Phi_2^\dagger \Phi_2 - \left[ m_{12}^2 \Phi_1^\dagger \Phi_2 + \text{h.c.} \right] + \frac{1}{2} \lambda_1 \left( \Phi_1^\dagger \Phi_1 \right)^2 + \frac{1}{2} \lambda_2 \left( \Phi_2^\dagger \Phi_2 \right)^2 \\ & + \lambda_3 \left( \Phi_1^\dagger \Phi_1 \right) \left( \Phi_2^\dagger \Phi_2 \right) + \lambda_4 \left( \Phi_1^\dagger \Phi_2 \right) \left( \Phi_2^\dagger \Phi_1 \right) + \left\{ \frac{1}{2} \lambda_5 \left( \Phi_1^\dagger \Phi_2 \right)^2 + \left[ \lambda_6 \left( \Phi_1^\dagger \Phi_1 \right) \right. \right. \\ & \left. \left. + \lambda_7 \left( \Phi_2^\dagger \Phi_2 \right) \right] \left( \Phi_1^\dagger \Phi_2 \right) + \text{h.c.} \right\}, \end{aligned} \quad (2.2)$$

where all the couplings are assumed to be real. The  $\mathbb{Z}_2$  symmetry implies  $\lambda_6 = \lambda_7 = 0$ . However, the term proportional to  $m_{12}^2$ , which softly breaks  $\mathbb{Z}_2$  can be non zero to keep the quartic coupling  $\lambda_1$  below perturbativity limit [1, 20]. Parameterizing the doublets as  $\Phi_j = (\phi_j^+, (v_j + \phi_j^r + i\phi_j^i)/\sqrt{2})^T$ , we obtain the five physical massive states  $A$ ,  $h$ ,  $H$ ,  $H^\pm$  in terms of the two diagonalizing angles  $\alpha$  and  $\beta$ :

$$\begin{aligned} A &= -s_\beta \phi_1^i + c_\beta \phi_2^i, & H^+ &= -s_\beta \phi_1^+ + c_\beta \phi_2^+, \\ h &= -s_\alpha \phi_1^r + c_\alpha \phi_2^r, & H &= c_\alpha \phi_1^r + s_\alpha \phi_2^r, \end{aligned} \quad (2.3)$$

where  $s_\alpha$  and  $c_\beta$  stand for  $\sin \alpha$  and  $\cos \beta$ , etc. The CP-even state  $h$  corresponds to the SM-like Higgs with mass  $M_h = 125$  GeV. Furthermore we look for the mass hierarchy  $M_A < M_h < M_H \simeq M_{H^\pm}$  which can be realised by setting  $\lambda_4 + \lambda_5 \approx 0$ . The SM-like Higgs couples to the pseudoscalar with strength  $\lambda_{hAA} = -(\lambda_3 + \lambda_4 - \lambda_5)v$ , where  $v = \sqrt{v_1^2 + v_2^2} = 246$  GeV.

The Yukawa Lagrangian of Eq.(2.1) can be rewritten in terms of the physical Higgs bosons,  $h, H, A$  and  $H^\pm$ :

$$\begin{aligned} \mathcal{L}_{\text{Yukawa}}^{\text{Physical}} = & - \sum_{f=u,d,\ell} \frac{m_f}{v} \left( \xi_h^f \bar{f} h f + \xi_H^f \bar{f} H f - i \xi_A^f \bar{f} \gamma_5 A f \right) \\ & - \left\{ \frac{\sqrt{2} V_{ud}}{v} \bar{u} \left( m_u \xi_A^u P_L + m_d \xi_A^d P_R \right) H^+ d + \frac{\sqrt{2} m_l}{v} \xi_A^l \bar{v}_L H^+ l_R + \text{h.c.} \right\}, \end{aligned} \quad (2.4)$$

where  $f$  runs over all of the quarks and charged leptons, and  $u$ ,  $d$ , and  $l$  refer to the up-type quarks, down-type quarks, and charged leptons, respectively. The multiplicative factors of

	$\xi_h^u$	$\xi_h^d$	$\xi_h^\ell$	$\xi_H^u$	$\xi_H^d$	$\xi_H^\ell$	$\xi_A^u$	$\xi_A^d$	$\xi_A^\ell$
Type-X	$c_\alpha/s_\beta$	$c_\alpha/s_\beta$	$-s_\alpha/c_\beta$	$s_\alpha/s_\beta$	$s_\alpha/s_\beta$	$c_\alpha/c_\beta$	$\cot \beta$	$-\cot \beta$	$\tan \beta$

**Table 1.** The multiplicative factors of Yukawa interactions in type X 2HDM

the Yukawa couplings, *i.e.*  $\xi_h^f$ ,  $\xi_H^f$  and  $\xi_A^f$  are given in Table 1. For  $\sin(\beta - \alpha) \approx 1$  the Yukawa coupling with the SM-like Higgs ( $h$ ) are similar to that of the SM. In any type of the 2HDM, the couplings of scalars with a pair of gauge bosons are given by [1, 2, 21]:

$$g_{hVV} = \sin(\beta - \alpha)g_{hVV}^{\text{SM}}, \quad g_{HVV} = \cos(\beta - \alpha)g_{hVV}^{\text{SM}}, \quad g_{AVV} = 0, \quad (2.5)$$

where  $V = Z, W^\pm$ . The couplings of  $Z$  boson with the neutral scalars are,

$$hAZ_\mu : \frac{g_Z}{2} \cos(\beta - \alpha)(p + p')_\mu, \quad HAZ_\mu : -\frac{g_Z}{2} \sin(\beta - \alpha)(p + p')_\mu, \quad (2.6)$$

where  $p_\mu$  and  $p'_\mu$  are outgoing four-momenta of the first and the second scalars, respectively, and  $g_Z = g_W / \cos \theta_W$ .

For reasons already stated, we are concerned with the region corresponding to  $\tan \beta \equiv v_2/v_1 \gg 1$ . This is because the contribution to the muon  $g - 2$  coming from the Barr-Zee [22] two-loop diagrams can be substantial with a light pseudoscalar  $A$  and  $\tau$  running in the loops. Constraints on 2HDM parameter space coming from  $(g - 2)_\mu$  have been analyzed in Refs. [4, 5, 10, 11, 23–30] and it was shown in the updated analysis [6] that light  $A$  in Type-X 2HDM can explain  $(g - 2)_\mu$  at  $2\sigma$  while evading collider as well as precision data constraints. While it is true that in the Type-II 2HDM a light pseudoscalar can explain the  $(g - 2)_\mu$  anomaly, there the lower bound on the charged Higgs mass is  $M_{H^\pm} > 580$  GeV coming from the  $B \rightarrow X_s \gamma$  measurement [31]. Such a heavy charged Higgs is not compatible with the requirement of a light pseudoscalar [4]. Similarly, in Type-I and Type-Y 2HDM, too, a very light pseudoscalar and its enhanced coupling with the muons are not consistent, since that would also imply comparably strong coupling to at least one type of quarks, leading to unacceptably large  $A$  production at hadron colliders. Beside those models where the  $A$  couples to muons proportionally to  $\cot \beta$  cannot explain  $(g - 2)_\mu$ , since  $\tan \beta \leq 1$  is disfavoured by a number of considerations. It is only in the Type-X that a light  $A$  can have enhanced coupling to the  $\mu$  and the  $\tau$ , concomitantly suppressed coupling to all quarks, and all phenomenological and other theoretical constraints (vacuum stability, perturbativity etc.) duly satisfied [32]. Keeping this in mind, we proceed to find a strategy for reconstructing  $M_A$  at the LHC.

### 3 Signal of a light $A$ : An analysis for the LHC

The light pseudoscalar in Type-X 2HDM can be produced at the LHC via associated production along with the SM Higgs and also via the decay of the SM like Higgs. The associated production is proportional to  $\cos^2(\beta - \alpha)$  and is suppressed for  $(\beta - \alpha) \simeq \pi/2$ , leaving  $h \rightarrow AA$  as the dominant production mode for the pseudoscalar. The pseudoscalar is lepto-philic and almost exclusively decays to  $\tau$  lepton for large  $\tan \beta$  with a very small

Parameters	$M_A$ (GeV)	$\tan \beta$	$\cos(\beta - \alpha)$	$\lambda_{hAA}/v$
BP1	50	60	0.03	0.02
BP2	60	60	0.03	0.03

**Table 2.** Benchmark points for studying the discovery prospects of light pseudoscalar in Type X 2HDM model at 14 TeV run of LHC.  $\lambda_{hAA}$  is in units of  $v = 246$  GeV.

branching ratio to di-muon ( $BR(A \rightarrow \mu\mu) \simeq (m_\mu/m_\tau)^2 \simeq 0.35\%$ ). This will lead to copious production of four- $\tau$  events ( $AA \rightarrow \tau^+\tau^-\tau^+\tau^-$ ), the characteristic Type-X signal which was analyzed in detail in Refs. [5, 15–17]. Since the decay of the  $\tau$  involves neutrinos, full reconstruction of the four- $\tau$  system is not possible which rules out any possibility of identifying a resonance peak. On the other hand if we consider the decay  $AA \rightarrow \mu^+\mu^-\tau^+\tau^-$  it is straightforward to identify the events owing to clean di-muon invariant mass ( $M_{\mu\mu}$ ) peak at  $M_A$  which will be the ‘smoking gun’ signal for a light spin-0 resonance. We show later that, in spite of the limited branching ratio for  $A \rightarrow \mu^+\mu^-$ , the  $2\mu\ 2\tau$  final state can identify the  $A$  peak well within the luminosity reach of the 14 TeV LHC.

The signal we are exploring contains a pair of oppositely charged muons with exactly two  $\tau$ -tagged jets produced via :

$$pp \rightarrow h \rightarrow AA \rightarrow \mu^+\mu^- \tau^+\tau^- \rightarrow \mu^+\mu^- j_\tau j_\tau + \cancel{E}_T, \quad (3.1)$$

where  $j_\tau$  is a  $\tau$ -tagged jet as a result of hadronic  $\tau$ -decay. The NNLO cross section for the Higgs production via gluon fusion at 14 TeV LHC is 50.35 pb [33].

The Type-X 2HDM model have been encoded using **FeynRules** [34, 35] in order to generate the model files for implementation in **MadGraph5\_aMC@NLO** [36, 37] which was used for computing the required cross-sections and generating events for collider analyses.

We have chosen the benchmark points (BP) given in Table 2 for our analysis. As we have explained in the previous section, we want a light pseudoscalar which can explain the muon  $g - 2$  anomaly at  $2\sigma$ . The benchmark points in the parameter space used here, corresponding to  $M_A = 50, 60$  GeV, are consistent with all phenomenological constraints. They also satisfy theoretical constraints such as perturbativity and a stable electroweak vacuum [4]. The signal of a light  $A$ , which is our main focus here, does not depend on  $M_H$  or  $M_{H^\pm}$ . For both of our benchmark points, each of these masses is 200 GeV. For the chosen benchmark scenarios, the branching ratio of Higgs to  $AA$  is  $BR(h \rightarrow AA) \simeq 15\%$  which is well below the upper limit of about 23% [38] on any non-standard decay branching ratio (BR) of the SM-like Higgs boson. The choice of  $\tan \beta$  ensures that the lepton universality bounds originating from  $Z$  and  $\tau$  decays are satisfied [6].

### 3.1 Backgrounds

The major backgrounds to our signal process :  $\mu^+\mu^- j_\tau j_\tau$  come from the following channels (A)  $pp \rightarrow \mu^+\mu^- + jets$ , (B)  $pp \rightarrow VV + jets$  ( $V = Z, W, \gamma^*$ ) and (C)  $pp \rightarrow t\bar{t} + jets$ . All the background events are generated with two additional partons and the events are matched up to two jets using MLM matching scheme [39, 40] using the *shower- $k_T$*  algorithm with

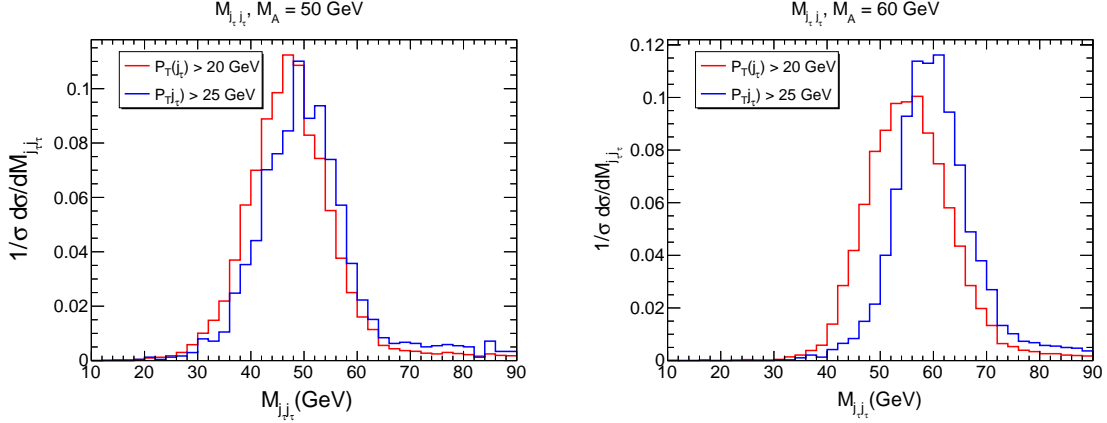


**Figure 1.** The invariant mass of the 2 tau-tagged jets for  $M_A = 50$  and  $M_A = 60$ . The figures illustrate how the higher  $p_T(j_\tau)$  threshold leads to more precise reconstruction of the peak at  $M_A$ .

$p_T$  ordered showers. We use NNLO production cross section for  $\mu^\pm \mu^\mp j j$  [41] and  $ZZ$  [42], whereas  $t\bar{t}$  production cross section is computed at N<sup>3</sup>LO [43].

Apart from these three backgrounds there exist other SM processes like  $VVV$ ,  $t\bar{t}V$  and  $W^\pm Z$  which in principle could fake the proposed signal ( $2\mu 2\tau$ ) [44]. However lower cross-section and the requirement of exactly two muons and two tau-tagged jets satisfying a tight invariant mass window around the pseudoscalar mass effectively eliminates the contribution from these additional channels.

### 3.2 Simulation and event selection

After generating both signal and background events with `MadGraph5_aMC@NLO`, we have used `PYTHIA6` [45] for the subsequent decay, showering and hadronization of the parton level events. Decay of  $\tau$  leptons is incorporated using `TAUOLA` [46] integrated in `MadGraph5_aMC@NLO`. Both one- and three-prong  $\tau$  decays have been included in our analysis. For event generation we have used the NN23L01 [47] parton distribution function and the default dynamic renormalisation and factorisation scales [48] in `MadGraph5_aMC@NLO`. Finally, detector simulation was done using `Delphes3` [49]. Jets were reconstructed using the anti- $k_T$  algorithm [50] with  $R = 0.4$ . The  $\tau$ -tagging efficiency and mistagging efficiencies of the light jets as  $\tau$ -jets are incorporated in `Delphes3` as reported by the ATLAS collaboration [51]. We operate our simulation on the Medium tag point for which the tagging efficiency of 1-prong (3-prong)  $\tau$  decay is 70% (60%) and the corresponding mistagging rate is 1% (2%).

The hadronic decays of the  $\tau$  are associated with some missing transverse energy in the events. For the signal events the  $\tau$  leptons originate from the decay of a light pseudoscalar ( $A$ ) with mass 50 or 60 GeV. Hence, if the  $p_T$  of the  $\tau$ -tagged jet has to be very close to  $m_A/2$ , the corresponding missing energy in the final state is suppressed. The invariant mass of the  $\tau$ -tagged jets will thus peak very close to the parent mass. In Figure 1 we substantiate this claim by plotting the invariant mass of the  $j_\tau j_\tau$  system for two different jet  $p_T$  thresholds. One can clearly see that for  $p_T(j_\tau) > 25$  GeV the invariant mass peaks

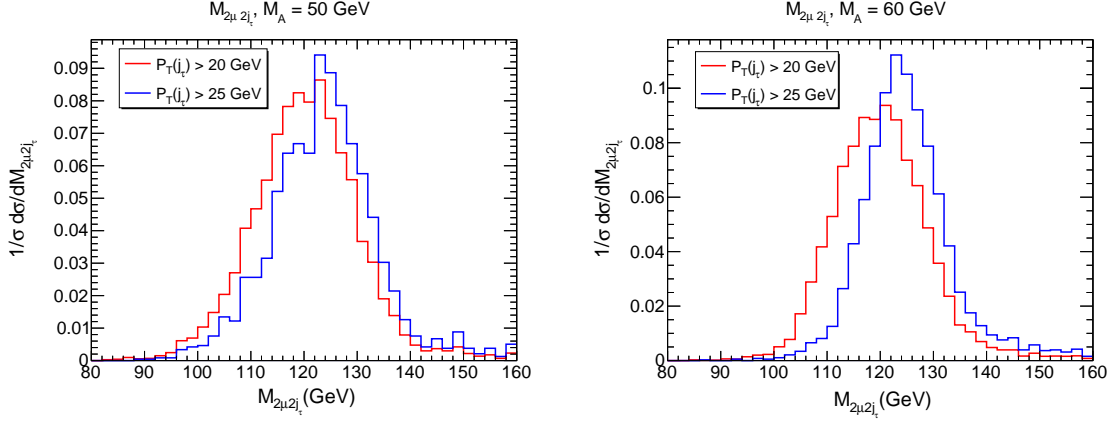


**Figure 2.** The invariant mass of the  $2\mu$  and 2 tau-tagged jets for  $M_A = 50$  and  $M_A = 60$ . The figures illustrate how the higher  $p_T(j_\tau)$  threshold leads to more precise reconstruction of the peak at  $M_h = 125$  GeV.

at the parent pseudoscalar mass, whereas  $M(j_\tau j_\tau)$  is peaking at a lower value than  $M_A$  for  $p_T(j_\tau) > 20$  GeV. Also the invariant mass peak is sharper for the higher  $p_T$  threshold. The four-body invariant mass  $M_{2\mu 2j_\tau}$  also shows the same features and peaks close to  $M_h = 125$  GeV as depicted in Figure. 2. It is evident that these variables can be very efficient in minimizing the background events.

We use the following selection cuts to select our signal and reduce the accompanying backgrounds:

- **Preselection Cuts:** We require the final state to have two oppositely charged muons of minimum  $p_T > 10$  GeV and  $|\eta| < 2.5$ . We also require two tau-tagged jets ( $j_\tau$ ) of minimum  $p_T$ ,  $p_T(j_\tau) > 20, 25$  GeV within  $|\eta| < 2.5$ .
- The invariant mass of the di-muon system ( $M_{\mu\mu}$ ) satisfies the window,

$$|M_{\mu\mu} - M_A| < 7.5 \text{ GeV}.$$

- The invariant mass of the two tau-tagged jets ( $M_{j_\tau j_\tau}$ ) satisfies:
  - for  $p_T(j_\tau) > 20$  GeV :  $(M_A - 20) < M_{j_\tau j_\tau} < (M_A + 10)$  GeV
  - for  $p_T(j_\tau) > 25$  GeV :  $|M_{j_\tau j_\tau} - M_A| < 15$  GeV.

- The invariant mass of two muons and two taujets ( $M_{2\mu 2j_\tau}$ ) lies within the range :
  - for  $p_T(j_\tau) > 20$  GeV :  $(M_h - 20) < M_{2\mu 2j_\tau} < (M_h + 10)$  GeV.
  - for  $p_T(j_\tau) > 25$  GeV :  $|M_{2\mu 2j_\tau} - M_h| < 15$  GeV.

Notice that we have taken asymmetric cut-windows with respect to  $M_A$  for  $M_{j_\tau j_\tau}$  and  $M_{2\mu 2j_\tau}$  for  $p_T(j_\tau) > 20$  GeV and symmetric ones for  $p_T(j_\tau) > 25$  GeV. This has to do with the fact that for lower  $p_T(j_\tau)$  cut, the invariant mass peaks at a lower value compared to the parent mass.

Cuts	Signal	$pp \rightarrow \mu^+ \mu^- + jets$	$pp \rightarrow VV + jets$	$pp \rightarrow t\bar{t} + jets$
$p_T(j_\tau) > 20 \text{ GeV}$				
Preselection	858 (1480)	41041 (41041)	107890 (107890)	14486 (14486)
$ M_{\mu\mu} - M_A  < 7.5 \text{ GeV}$	836 (1430)	909 (779)	1189 (1325)	1637 (1697)
$M_{j_\tau j_\tau} > M_A - 20 \text{ \&}$ $M_{j_\tau j_\tau} < M_A + 10 \text{ GeV}$	760 (1336)	130 (390)	307 (654)	330 (419)
$M_{2\mu 2j_\tau} > M_h - 20 \text{ \&}$ $M_{2\mu 2j_\tau} < M_h + 10 \text{ GeV}$	698 (1283)	$< 130 (< 390)^*$	81 (109)	65 (51)
$p_T(j_\tau) > 25 \text{ GeV}$				
Preselection	277 (493)	28833 (28833)	75209 (75209)	11629 (11629)
$ M_{\mu\mu} - M_A  < 7.5 \text{ GeV}$	269 (475)	649 (390)	794 (924)	1324 (1396)
$ M(j_\tau j_\tau) - M_A  < 15 \text{ GeV}$	228 (420)	$< 649 (130)$	112 (416)	182 (196)
$ M_{2\mu 2j_\tau} - M_h  < 15 \text{ GeV}$	211 (410)	$< 649 (< 130)^*$	20 (15)	27 (27)

**Table 3.** Cut flow table for signal BP1(BP2) and different background processes with two different set of  $p_T(j_\tau)$  cuts as described in Section 3.2. The number of events are computed with integrated luminosity of  $3000 \text{ fb}^{-1}$ . The number of background events also depends on benchmark points as  $M_A$  changes.

## 4 Results and Discussion

In Table 3, we present the cut flow for the signal and the various backgrounds for the benchmark points BP1 (BP2) where the number of events are calculated at the integrated luminosity of  $3000 \text{ fb}^{-1}$ . Note that some of the background events are estimated as upper bound (marked by an asterisk), as the number of simulated events passing the cuts drop down to very small values at some point in the cut flow table, even after simulating with  $2 \times 10^7$  events for the background analysis. Since we adopt the Medium Tag point for tau-tagging, the mistagging rate for a pair of light jets is  $\sim 10^{-4}$ . This, along with a tight invariant mass window around  $M_A$  helps to get rid of a major fraction of the various background channels. Demanding that  $|M_{\mu\mu} - M_A| < 7.5 \text{ GeV}$  should take care of the  $Z$  contribution in  $pp \rightarrow \mu^+ \mu^- + jets$  and  $pp \rightarrow VV + jets$ . After the cut on  $M_{\mu\mu}$  only a feeble contribution from the photon (and partly off-shell  $Z$ ) continuum can contribute in the  $pp \rightarrow \mu^+ \mu^- + jets$  channel.

We compute the statistical significance by using the formula,  $\mathcal{S} = \sqrt{2 [(S+B) \ln(1 + \frac{S}{B}) - S]}$  where  $S(B)$  are number of signal (background) events which survive the cuts. In Figure 3 we have plotted the significance  $\mathcal{S}$  as a function of integrated luminosity for both the benchmark points where BP1(BP2) corresponds to  $M_A = 50(60) \text{ GeV}$ . For BP1 it is possible to reach  $5\sigma$  sensitivity at integrated luminosity of  $70(400) \text{ fb}^{-1}$  with  $p_T(j_\tau) > 20(25) \text{ GeV}$ . For BP2 the  $5\sigma$  sensitivity is achievable at  $40(125) \text{ fb}^{-1}$  integrated luminosity. Increasing the minimum  $p_T(j_\tau)$  from 20 GeV to 25 GeV results in better invariant mass peaks

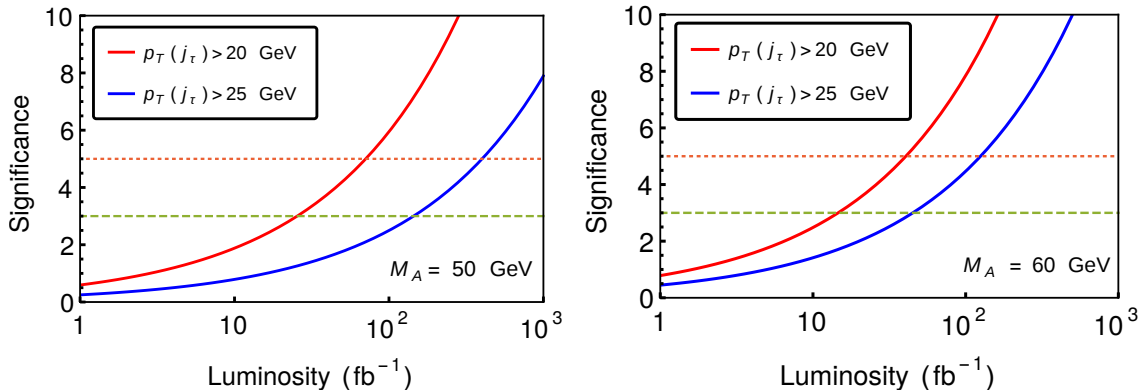


**Figure 3.** Discovery potential of the light pseudoscalar decaying to di-muon and di-tau channel using invariant mass variables for BP1(left panel) and BP2(right panel) at 14 TeV LHC.

but provides fewer number of events which decreases the discovery prospect of the model. However the luminosity requirement is well within the reach of high luminosity run at the LHC.

The benchmarks chosen in this work allowing for the  $BR(h \rightarrow AA) \sim 15\%$  are close to the borderline of the exclusion limit on  $\sigma(h) \times BR(h \rightarrow AA) \times BR(A \rightarrow \mu\mu)^2$  [52, 53], when this is translated for  $A \rightarrow 2\mu 2\tau$ . However, one can still allow for a lower branching ratio for  $h \rightarrow AA$ , for example, close to 10%, which keeps one well within the exclusion limit, satisfying all the other constraints. This would entail the required luminosity for a  $5\sigma$  discovery to be nearly double the values quoted above.

If  $A$  were a scalar instead of a pseudoscalar, then it would also have decays into  $W^*W^*$  and  $Z^*Z^*$  competing with the  $\mu^+\mu^-$  mode. The non-observation of such final states, even with accumulating luminosity, should act as a pointer to the  $CP$ -odd nature of  $A$ . Secondly, the presence of such channels eats into the branching ratio of the  $A$ , and suppresses the  $\mu^+\mu^-$  channel rate, reducing it below detectability. The fact that we can reconstruct the  $A$  via the  $\mu\mu$  peak (which is the main point we make in this work) owes itself to the non-negligible branching ratio for this mode, which would not have been possible if it were a scalar instead of a pseudoscalar.

On the other hand, if  $A$  were a superposition of a scalar and a pseudoscalar field (i.e. if  $CP$  were violated), then the taus coming from the decay of the other  $A$  would consist of unequal admixtures of right- and left-polarised states (both for  $\tau^-$  and  $\tau^+$ ). In principle, suitable triple products of vectors constructed out of the tau-decay products would have asymmetric distributions if  $CP$ -violation had taken place. However, the construction of such  $CP$ -asymmetric triple products would have required us to reconstruct the taus fully. This would warrant the so-called collinear approximation, where the  $\tau$ , the decay product jet and a neutrino would all move along the same straight line. This approximation is valid if the tau has an energy of at least about 40 GeV. In our case, for a light (50 – 60 GeV)  $A$  this energy is not possessed by the taus, and thus their reconstruction is not reliable. Therefore, while one can distinguish a pure pseudoscalar from a pure scalar in this channel, identifying a  $CP$ -admixture is difficult.

It is possible to search for the heavy scalar  $H$  and the pseudoscalar using the  $pp \rightarrow Z \rightarrow HA$  production channel. In principle, this enables one to reconstruct the  $H$  mass. However, this associated production rate will be two orders of magnitude smaller than the rate for  $pp \rightarrow h \rightarrow AA$ , principally due to the large Higgs production rate from gluon fusion. Nevertheless, if one notices a low-mass  $\mu^+\mu^-$  peak from  $A$ , one can look for a tau-pair peak simultaneously in such events. It is relatively easy to reconstruct tau-leptons from the tau-jets in such a case, since these taus are quite energetic and the collinear approximation [18] will work for them. Thus, in association with a light  $A$  constructed in the way suggested in our paper, a heavy  $H$  can also be looked for, albeit at higher luminosity.

In addition, a light  $A$  may of course be responsible for  $4\tau$  final states. Some channels leading to such a final state have been analyzed in [5, 16, 17]. We observe that the  $\geq 3\tau$  final state fares better in terms of the statistical significance owing to the dominant branching ratio of  $A \rightarrow \tau^+\tau^-$  as compared to the much smaller branching ratio of  $A \rightarrow \mu^+\mu^-$ . For instance, for a  $5\sigma$  discovery of  $M_A = 60$  GeV with  $M_H = 200$  GeV, the required luminosity is approximately  $70 \text{ fb}^{-1}$  as against  $218 \text{ fb}^{-1}$  for the  $2\mu 2\tau$  final state. However, the di-muon pair is a lot cleaner to reconstruct, and gives an accurate handle on the mass determination for the parent pseudoscalar. Thus the  $2\mu 2\tau$  state is more informative when it comes to “identifying” the pseudoscalar.

## 5 Summary and Conclusion

While the Type-X 2HDM admits of a light pseudoscalar, the explicit reconstruction of its mass is a challenging task. We propose to meet this challenge by making use of the small but non-negligible branching ratio for  $A \rightarrow \mu^+\mu^-$ , especially in the region of the parameter space, which best explains the muon anomalous magnetic moment. We have studied the channel  $pp \rightarrow h \rightarrow AA \rightarrow \mu^+\mu^- \tau^+\tau^-$ , with the taus decaying into a jet each. The  $\mu^+\mu^-$  pair shows a conspicuous invariant mass peak at  $M_A$ . Besides, an appropriate  $p_T$ -cut on the tau-tagged jets also creates a  $j_\tau j_\tau$  mass distribution that has a peak in the neighbourhood of  $M_A$ . A proper window demanded of the latter invariant mass helps the effective tagging and background reduction for the  $\mu^+\mu^-$  peak. We find that, for  $M_A$  between 50 and 60 GeV,  $M_A$  can be reconstructed in this manner, with statistical significance of 4-5  $\sigma$  with an integrated luminosity not far exceeding  $100 \text{ fb}^{-1}$  in the 14 TeV run.

## 6 Acknowledgements

BM thanks Korea Institute for Advanced Study for hospitality while this project was initiated. This work was partially supported by funding available from the Department of Atomic Energy, Government of India, for the Regional Centre for Accelerator-based Particle Physics (RECAPP), Harish-Chandra Research Institute. SD thanks N. Chakrabarty for helpful discussions. The authors acknowledge the use of the cluster computing setup available at RECAPP and at the High Performance Computing facility of HRI.

## References

- [1] J. F. Gunion, H. E. Haber, G. L. Kane, and S. Dawson, *Front. Phys.* **80**, 1 (2000).
- [2] A. Djouadi, *Phys. Rept.* **459**, 1 (2008), [hep-ph/0503173](#).
- [3] G. C. Branco, P. M. Ferreira, L. Lavoura, M. N. Rebelo, M. Sher, and J. P. Silva, *Phys. Rept.* **516**, 1 (2012), [1106.0034](#).
- [4] A. Broggio, E. J. Chun, M. Passera, K. M. Patel, and S. K. Vempati, *JHEP* **11**, 058 (2014), [1409.3199](#).
- [5] E. J. Chun, Z. Kang, M. Takeuchi, and Y.-L. S. Tsai, *JHEP* **11**, 099 (2015), [1507.08067](#).
- [6] E. J. Chun and J. Kim, *JHEP* **07**, 110 (2016), [1605.06298](#).
- [7] P. Bandyopadhyay, C. Coriano, and A. Costantini, *JHEP* **09**, 045 (2015), [1506.03634](#).
- [8] P. Bandyopadhyay, C. Coriano, and A. Costantini, *JHEP* **12**, 127 (2015), [1510.06309](#).
- [9] D. Goncalves and D. Lopez-Val, *Phys. Rev.* **D94**, 095005 (2016), [1607.08614](#).
- [10] K.-m. Cheung, C.-H. Chou, and O. C. W. Kong, *Phys. Rev.* **D64**, 111301 (2001), [hep-ph/0103183](#).
- [11] K. Cheung and O. C. W. Kong, *Phys. Rev.* **D68**, 053003 (2003), [hep-ph/0302111](#).
- [12] F. Jegerlehner and A. Nyffeler, *Phys. Rept.* **477**, 1 (2009), [0902.3360](#).
- [13] M. Lisanti and J. G. Wacker, *Phys. Rev.* **D79**, 115006 (2009), [0903.1377](#).
- [14] J. Cao, P. Wan, L. Wu, and J. M. Yang, *Phys. Rev.* **D80**, 071701 (2009), [0909.5148](#).
- [15] S. Su and B. Thomas, *Phys. Rev.* **D79**, 095014 (2009), [0903.0667](#).
- [16] S. Kanemura, K. Tsumura, and H. Yokoya, *Phys. Rev.* **D85**, 095001 (2012), [1111.6089](#).
- [17] S. Kanemura, K. Tsumura, K. Yagyu, and H. Yokoya, *Phys. Rev.* **D90**, 075001 (2014), [1406.3294](#).
- [18] D. L. Rainwater, D. Zeppenfeld, and K. Hagiwara, *Phys. Rev.* **D59**, 014037 (1998), [hep-ph/9808468](#).
- [19] S. L. Glashow and S. Weinberg, *Phys. Rev. D* **15**, 1958 (1977), URL <https://link.aps.org/doi/10.1103/PhysRevD.15.1958>.
- [20] J. F. Gunion and H. E. Haber, *Phys. Rev.* **D67**, 075019 (2003), [hep-ph/0207010](#).
- [21] S. Kanemura, H. Yokoya, and Y.-J. Zheng, *Nucl. Phys.* **B886**, 524 (2014), [1404.5835](#).
- [22] S. M. Barr, E. M. Freire, and A. Zee, *Phys. Rev. Lett.* **65**, 2626 (1990), URL <https://link.aps.org/doi/10.1103/PhysRevLett.65.2626>.
- [23] A. Dedes and H. E. Haber, *JHEP* **05**, 006 (2001), [hep-ph/0102297](#).
- [24] M. Krawczyk (2001), [hep-ph/0103223](#).
- [25] M. Krawczyk, *Acta Phys. Polon.* **B33**, 2621 (2002), [hep-ph/0208076](#).
- [26] L. Wang and X.-F. Han, *JHEP* **05**, 039 (2015), [1412.4874](#).
- [27] V. Ilisie, *JHEP* **04**, 077 (2015), [1502.04199](#).
- [28] T. Abe, R. Sato, and K. Yagyu, *JHEP* **07**, 064 (2015), [1504.07059](#).
- [29] T. Han, S. K. Kang, and J. Sayre, *JHEP* **02**, 097 (2016), [1511.05162](#).

- [30] A. Cherchiglia, P. Kneschke, D. Stöckinger, and H. Stöckinger-Kim, JHEP **01**, 007 (2017), [1607.06292](#).
- [31] A. Abdesselam et al. (Belle), in *Proceedings, 38th International Conference on High Energy Physics (ICHEP 2016): Chicago, IL, USA, August 3-10, 2016* (2016), [1608.02344](#), URL <https://inspirehep.net/record/1479946/files/arXiv:1608.02344.pdf>.
- [32] F. Staub (2017), [1705.03677](#).
- [33] <https://twiki.cern.ch/twiki/bin/view/LHCPhysics/HiggsEuropeanStrategy>.
- [34] N. D. Christensen and C. Duhr, Comput. Phys. Commun. **180**, 1614 (2009), [0806.4194](#).
- [35] A. Alloul, N. D. Christensen, C. Degrande, C. Duhr, and B. Fuks, Comput. Phys. Commun. **185**, 2250 (2014), [1310.1921](#).
- [36] J. Alwall, M. Herquet, F. Maltoni, O. Mattelaer, and T. Stelzer, JHEP **06**, 128 (2011), [1106.0522](#).
- [37] J. Alwall, R. Frederix, S. Frixione, V. Hirschi, F. Maltoni, O. Mattelaer, H. S. Shao, T. Stelzer, P. Torrielli, and M. Zaro, JHEP **07**, 079 (2014), [1405.0301](#).
- [38] G. Aad et al. (ATLAS), JHEP **11**, 206 (2015), [1509.00672](#).
- [39] M. L. Mangano, M. Moretti, F. Piccinini, and M. Treccani, JHEP **01**, 013 (2007), [hep-ph/0611129](#).
- [40] S. Hoeche, F. Krauss, N. Lavesson, L. Lonnblad, M. Mangano, A. Schalicke, and S. Schumann, in *HERA and the LHC: A Workshop on the implications of HERA for LHC physics: Proceedings Part A* (2005), pp. 288–289, [hep-ph/0602031](#), URL [http://inspirehep.net/record/709818/files/arXiv:hep-ph\\_0602031.pdf](http://inspirehep.net/record/709818/files/arXiv:hep-ph_0602031.pdf).
- [41] S. Catani, L. Cieri, G. Ferrera, D. de Florian, and M. Grazzini, Phys. Rev. Lett. **103**, 082001 (2009), [0903.2120](#).
- [42] F. Cascioli, T. Gehrmann, M. Grazzini, S. Kallweit, P. Maierhöfer, A. von Manteuffel, S. Pozzorini, D. Rathlev, L. Tancredi, and E. Weihs, Phys. Lett. **B735**, 311 (2014), [1405.2219](#).
- [43] C. Muselli, M. Bonvini, S. Forte, S. Marzani, and G. Ridolfi, JHEP **08**, 076 (2015), [1505.02006](#).
- [44] Tech. Rep. CMS-PAS-HIG-16-036, CERN, Geneva (2017), URL <http://cds.cern.ch/record/2242956>.
- [45] T. Sjostrand, S. Mrenna, and P. Z. Skands, JHEP **05**, 026 (2006), [hep-ph/0603175](#).
- [46] S. Jadach, Z. Was, R. Decker, and J. H. Kuhn, Comput. Phys. Commun. **76**, 361 (1993).
- [47] R. D. Ball et al. (NNPDF), JHEP **04**, 040 (2015), [1410.8849](#).
- [48] ["http://cp3.irmp.ucl.ac.be/projects/madgraph/wiki/FAQ-General-13"](http://cp3.irmp.ucl.ac.be/projects/madgraph/wiki/FAQ-General-13).
- [49] J. de Favereau, C. Delaere, P. Demin, A. Giammanco, V. Lemaître, A. Mertens, and M. Selvaggi (DELPHES 3), JHEP **02**, 057 (2014), [1307.6346](#).
- [50] M. Cacciari, G. P. Salam, and G. Soyez, JHEP **04**, 063 (2008), [0802.1189](#).
- [51] Tech. Rep. ATL-PHYS-PUB-2015-045, CERN, Geneva (2015), URL <https://cds.cern.ch/record/2064383>.

- [52] Tech. Rep. CMS-PAS-HIG-15-011, CERN, Geneva (2016), URL <https://cds.cern.ch/record/2128149>.
- [53] R. Aggleton, D. Barducci, N.-E. Bomark, S. Moretti, and C. Shepherd-Themistocleous, JHEP **02**, 035 (2017), [1609.06089](#).